Acta Oceanol. Sin., 2018, Vol. 37, No. 1, P. 40–49
DOI: 10.1007/s13131-018-1157-9
http://www.hyxb.org.cn
E-mail: hyxbe@263.net

Storm surge simulation along the Meghna estuarine area: an alternative approach

PAUL Gour Chandra[1]*, SENTHILKUMAR Sukumar[2], PRIA Rana[3]

[1] Department of Mathematics, University of Rajshahi, Rajshahi 6205, Bangladesh

[2] School of Mathematical Sciences, Universiti Sains Malaysia, Pulau Pinang-11800, Malaysia

[3] Mathematics Discipline, Khulna University, Khulna 9208, Bangladesh

Received 5 November 2016; accepted 22 June 2017

Abstract

In this study, numerical prediction of surges associated with a storm was made through the method of lines (MOL) in coordination with the newly proposed RKARMS (4, 4) method for the meghna estuarine region, along the coast of Bangladesh. For this purpose, the vertically integrated shallow water equations (SWEs) in Cartesian coordinates were firstly transformed into ordinary differential equations (ODEs) of initial valued, which were then soloved using the new RKARMS (4, 4) method. Nested grid technique was employed for resolving the complexities of the region of interest with minimum cost. Fresh water discharge through the lower Meghna River was taken into account along the north east corner of the innermost child scheme. Numerical experiments were performed with the severe cyclone on April 1991 that crossed the coast over the study area. Simulated results by the study were found to be in good agreement with some reported data and were found to compare well with the results obtained by the MOL in addition with the classical 4th order Runge-Kutta (RK (4, 4)) method and the standard finite difference method (FDM).

Key words: method of lines, storm surge, nested grid, finite difference method, RKARMS (4, 4) method, truncation errors

Citation: Paul Gour Chandra, Senthilkumar Sukumar, Pria Rana. 2018. Storm surge simulation along the Meghna estuarine area: an alternative approach. Acta Oceanologica Sinica, 37(1): 40–49, doi: 10.1007/s13131-018-1157-9

1 Introduction

New tasks and paradigms are emerging in surge analysis because of the availability of information technology and increased amount of support data for building nonlinear system models. Accurate precipitation forecasts essential in the prediction of water levels due to surge with numerical models have proved to be useful for disaster planning, coastal management and reduction of losses resulting from storm surges (e.g., Das, 1972; Paul et al., 2014), and research is still being carried out towards the same for finding out more accurate solution. However, designing of a novel technique is always desirable in research community and its development. The method of lines (MOL) is a well-established numerical procedure for the treatment of boundary value problems (BVPs) providing a mathematical description of space and time. The method has no relative convergence problem and numerical instability (Sun et al., 1993), which can be used for saving computational cost in solving partial differential equations (PDEs) (Paul et al., 2014). The method is more effective over the finite difference method (FDM) with regard to accuracy and computational cost (Sadiku and Garcia, 2000). In simulating Indonesian tsunami 2004 along the coastal belt of Peninsular Malaysia and Thailand, Ismail et al. (2007) used the MOL in coordination with the RK (4, 4) method to solve vertically integrated shallow water equations (SWEs). They found the MOL to be an effective algorithm for solving SWEs, and to be a suitable procedure for the analysis of long waves originated in the shallow water. Keeping the idea in mind, Paul et al. (2014) solved SWEs for foreseeing water levels along the coast of Bangladesh associated with the severe cyclone in April 1991. They also found the MOL to be suitable technique over the FDM in solving SWEs in terms of accuracy, stability, and central processing unit (CPU) time. The basic idea of the MOL for solving time dependent PDEs is to approximate the spatial partial derivatives to obtain a system of ordinary differential equations (ODEs) of initial valued in most cases and thereby to solve applying any well-developed time integrators. In solving SWEs by the MOL, Paul et al. (2014) applied the RK (4, 4) method, where they concluded that the efficiencey of the MOL solution can be enhanced by using any well–established time integrators.

It is to be noted here that one of the limitations in implementing the RK (4, 4) method is the absence of error estimation procedure in estimating numerical solutions (Yaacob and Sanugi, 1998). Several methods have been developed to overcome this weakness. Pioneering works in this regard are due to Merson (1957) and Fehlberg (1969). Many details in the process since then have been advanced through the investigations of Yaakub and Evans (Evans and Yaakub, 1995; Yaakub and Evans, 1999; Yaacob and Sanugi, 1998; Ponalagusamy and Senthilkumar, 2009; Senthilkumar, 2009). Recently Ponalagusamy and Senthilkumar (2009) proposed a novel fourth order embedded RKARMS (4, 4) method to solve the real time application problems efficiently in image processing under cellular neural network (CNN) model and algorithm based on Runge-Kuttaa (RK) arithmetic root mean square with error control in detail. A detailed illustration related to local truncation error (LTE), global truncation error (GTE), and error estimation (EE) and control for

*Corresponding author, E-mail: pcgour2001@yahoo.com

the method can be found in Senthilkumar (2009). Paul and Senthilkumar (2016) tested the efficiencey of the RKARMS (4, 4) method in investigating protoplanetary structure, where they found the results by the method to be insensitive of the choice of the end points.

In this paper, we intend to simulate surge (in the absence of astronomical tide) associated with a strom along the Meghna estuarine region of the coast of Bangladesh by the MOL in coordination with the RKARMS (4, 4) method and to see how this different approach compare the results obtained with other two established methods, namely the FDM and the MOL in coordination with RK (4, 4) method and some reproted results.

The remainder of the paper is organized as follows. Section 2 deals with the model of SWEs with boundary conditions. A short note on the novel RKARMS (4, 4) method is addressed in Section 3. Numerical procedures are detailed in Section 4. Simulated results and analysis are presented in Section 5, and conclusions are given in Section 6.

2 Basic equations

Prediction of water levels due to surge will be investigated based on the vertically integrated SWEs (Debsarma, 2009; Paul et al., 2014):

$$\frac{\partial \zeta}{\partial t}=-\frac{\partial}{\partial x}[(\zeta+h)u]-\frac{\partial}{\partial y}[(\zeta+h)v], \tag{1}$$

$$\frac{\partial u}{\partial t}=-u\frac{\partial u}{\partial x}-v\frac{\partial u}{\partial y}+fv-g\frac{\partial \zeta}{\partial x}+\frac{T_x}{\rho(\zeta+h)}-\frac{C_f u\left(u^2+v^2\right)^{1/2}}{\zeta+h}, \tag{2}$$

$$\frac{\partial v}{\partial t}=-u\frac{\partial v}{\partial x}-v\frac{\partial v}{\partial y}-fu-g\frac{\partial \zeta}{\partial y}+\frac{T_y}{\rho(\zeta+h)}-\frac{C_f v\left(u^2+v^2\right)^{1/2}}{\zeta+h}, \tag{3}$$

where x and y are coordinate axes directed towards the south and the east, respectively; u and v represent Reynolds averaged components of velocity in the directions of x and y, respectively; $\zeta(x, y, t)$ is the displaced level of the surface of the sea; $h(x, y)$ is the position of the sea bed; $f=2\Omega\sin\varphi$ is the Coriolis parameter, where $\Omega(=7.29\times10^{-5}$ rad/s) is the angular speed of the Earth rotation and φ is the latitude of the place, wherever necessary; g is the acceleration due to gravity; $\rho(=1.03\times10^3$ kg/m^3) is the density of the sea water, assumed to be homogeneous; C_f is the friction coefficient; (T_x, T_y) represents the components of wind stress.

In this study, surface stresses are parameterized by the conventional quadratic law:

$$(T_x, T_y)=\rho_a C_D(u_a^2+v_a^2)^{1/2}(u_a, v_a), \tag{4}$$

where C_D is the drag coefficient, ρ_a is the air density and u_a and v_a are the x and y components of surface wind, respectively. The surface wind field over the model domain is derived following Paul et al. (2014) from the empirical formula due to Jelesnianski (1965), which is given by

$$V_a=\begin{cases}V_0\sqrt{(r_a/R)^3} & \text{for all } r_a\leqslant R,\\ V_0\sqrt{(R/r_a)} & \text{for all } r_a>R,\end{cases} \tag{5}$$

where V_0 represents the maximum sustained wind at the radial distance R from the eye of the cyclone and r_a is any radial distance from the eye at which the wind field is desired. It is to be noted here that the parameters involved in Eq. (5), namely R and V_0 are available during any storm along the region of interest at the Bangladesh Meteorological Department (BMD).

There are two types of boundaries in our model domain: closed and open boundaries. The normal component of the depth averaged velocity at the closed boundary (mainland and island boundaries) is set to zero and for open boundaries, a condition of radiation type is used to allow the disturbance, generated within the model area, to go out through the open boundary (Paul et al., 2016). Apart from the coast of Bangladesh, the boundaries are treated as straight lines in the open sea, which are given by (Roy, 1995)

$$\text{west boundary}\,(85°\text{E}): v+(g/h)^{1/2}\zeta=0, \tag{6}$$

$$\text{east boundary}\,(95°\text{E}): v-(g/h)^{1/2}\zeta=0, \tag{7}$$

$$\text{south boundary}\,(15°\text{N}): u-\left(\frac{g}{h}\right)^{1/2}\zeta=0. \tag{8}$$

3 A short note on RKARMS (4, 4) method

As in Paul and Senthilkumar (2016), the RKAM (4, 4) method can be written in the Butcher array form as

0				
$\frac{1}{2}$	$\frac{1}{2}$			
$\frac{1}{2}$	0	$\frac{1}{2}$		
1	0	0	1	0
	$\frac{1}{6}$	$\frac{1}{3}$	$\frac{1}{3}$	$\frac{1}{6}$

$$y_{n+1}=y_n+\frac{h}{3}\left(\frac{k_1+k_2}{2}+\frac{k_2+k_3}{2}+\frac{k_3+k_4}{2}\right), \tag{9}$$

where

$$\boldsymbol{k}_1=f(x_n, y_n),$$

$$\boldsymbol{k}_2=f\left(x_n+\frac{h}{2}, y_n+\frac{h\boldsymbol{k}_1}{2}\right),$$

$$\boldsymbol{k}_3=f\left(x_n+\frac{h}{2}, y_n+\frac{h\boldsymbol{k}_2}{2}\right),$$

$$\boldsymbol{k}_4=f(x_n+h, y_n+h\boldsymbol{k}_3).$$

The fourth order RK root mean square (RKRMS (4, 4)) method with Butcher array can be written in the modified form as (Paul and Senthilkumar, 2016)

0				
$\frac{1}{2}$	$\frac{1}{2}$			
$\frac{1}{2}$	0	$\frac{1}{2}$		
1	0	0	1	
	$\frac{1}{3}$	$\frac{1}{3}$	$\frac{1}{3}$	

The RKRMS (4, 4) method due to Evans and Yaakub (1995) is

given by

$$y_{n+1}=y_n+\frac{h}{3}\left[\sqrt{\frac{k_1^2+k_2^2}{2}}+\sqrt{\frac{k_2^2+k_3^2}{2}}+\sqrt{\frac{k_3^2+k_4^2}{2}}\right], \tag{10}$$

where

$$\begin{aligned}
&k_1=f(x_n,y_n),\\
&k_2=f\left(x_n+\frac{1}{2}h,y_n+\frac{1}{2}hk_1\right),\\
&k_3=f\left(x_n+\frac{1}{2}h,y_n+\frac{1}{16}hk_1+\frac{7}{16}hk_2\right),\\
&k_4=f\left(x_n+h,y_n+\frac{1}{8}hk_1-\frac{17}{56}hk_2+\frac{33}{28}hk_3\right).
\end{aligned}$$

It is well-known that combination of RKAM (4, 4) and RKRMS (4, 4) (Eqs (9) and (10)) leads to give a new formation of RKARMS (4, 4), and is formulated by Ponalagusamy and Senthilkumar (2009) as

$$\begin{aligned}
&k_1=f(x_n,y_n)=k_1^*,\\
&k_2=f(x_n+\frac{h}{2},y_n+\frac{hk_1}{2})=k_2^*,\\
&k_3=f(x_n+\frac{h}{2},y_n+\frac{hk_2}{2}),\\
&k_4=f(x_n+h,y_n+hk_3),\\
&k_3=f(x_n+\frac{1}{2}h,y_n+\frac{1}{16}hk_1+\frac{7}{16}hk_2)=k_3^*,\\
&k_4=f(x_n+h,y_n+\frac{1}{8}hk_1+\frac{17}{56}hk_2+\frac{33}{28}hk_3)=k_4^*,
\end{aligned}$$

$$y_{n+1}=y_n+\frac{h}{3}\left[\frac{k_1+k_2}{2}+\frac{k_2+k_3}{2}+\frac{k_3+k_4}{2}\right], \tag{11}$$

$$y_{n+1}^*=y_n+\frac{h}{3}\left[\sqrt{\frac{k_1^{*2}+k_2^{*2}}{2}}+\sqrt{\frac{k_2^{*2}+k_3^{*2}}{2}}+\sqrt{\frac{k_3^{*2}+k_4^{*2}}{2}}\right]. \tag{12}$$

As in Paul and Senthilkumar (2016), the embedded RKARMS (4, 4) method can be expressed in array form as

0			
$\frac{1}{2}$	$\frac{1}{2}$		
$\frac{1}{2}$	0	$\frac{1}{2}$	
1	0	0	1
	…	…	…
	…	…	…
$\frac{1}{2}$	$\frac{1}{16}$	$\frac{7}{16}$	
1	$\frac{1}{8}$	$\frac{-17}{56}$	$\frac{33}{28}$
	$\frac{1}{3}$	$\frac{1}{3}$	$\frac{1}{3}$
	$\frac{1}{3}$	$\frac{1}{3}$	$\frac{1}{3}$
	E^{T}		

where

$$b^{\mathrm{T}}=y_{n+1}^{AM}=y_n+\frac{h}{3}\left[\frac{k_1+k_2}{2}+\frac{k_2+k_3}{2}+\frac{k_3+k_4}{2}\right], \tag{13}$$

$$\hat{b}^{\mathrm{T}}=y_{n+1}^{RMS}=y_n+\frac{h}{3}\left[\sqrt{\frac{k_1^{*2}+k_2^{*2}}{2}}+\sqrt{\frac{k_2^{*2}+k_3^{*2}}{2}}+\sqrt{\frac{k_3^{*2}+k_4^{*2}}{2}}\right], \tag{14}$$

and the estimation of the LTE, $E^{\mathrm{T}}=\left|b^{\mathrm{T}}-\hat{b}^{\mathrm{T}}\right|$. In the RKARMS (4, 4) method, four stages are required to obtain the solution, which share the same set of vectors k_1 and k_2 using b^{T} and $\hat{b}^{\mathrm{T}}$ approximately, but k_3 and k_4 use b^{T} while k_3^* and k_4^* use $\hat{b}^{\mathrm{T}}$. The derivation of the LTE and EE for the RKARMS (4, 4) method can be found in detail in Senthilkumar (2009) and Paul and Senthilkumar (2016).

4 Numerical procedures

4.1 *Set up of nested numerical schemes*

The meghna estuary of Bangladesh is the world's most vulnerable region because of the existence of thickly populated big and small islands, complex land-sea interface (Fig. 1), flat shallow bed, and shape of the coast (Roy, 1995; Roy et al., 1999). Besides, storm surges in the region of interest are amplified by some other factors found in Paul et al. (2016). An accurate prediction of surge levels for this region necessities proper understanding of the factors and their accurate incorporation. A use of high resolution of grids may be a solution in this regard (Paul and Ismail, 2012). However, with the use of the high resolution for the hole domain, as we will see later, computational cost may be increased tremendously, which is undesirable for a model of practical forecasting (Roy et al., 1999; Paul et al., 2014). The nested grid method is thought to be a probable solution in this regard (Paul and Ismail, 2012, 2013). The features of these schemes are that they allow specification of a desired resolution in a region of interest with lower resolution elsewhere (Paul et al., 2016). In our study, a high-resolution fine mesh numerical scheme (FMNS), capable of incorporating all major islands, is nested into a coarse mesh numerical scheme (CMNS). To take into account the complex land-sea interface and to incorporate bottom topographic details, a very high resolution numerical scheme (VFMNS) covering our region of concern is again nested into the FMNS. Some basic information on the schemes is given in Table 1. The coupling of our used schemes is made following the procedure addressed in Paul et al. (2016).

The Meghna River fresh water discharge is considered along the northern boundary of the VFMNS between 90.4°–90.6°E (Fig. 1) and the fresh water discharge of the river is incorporated according to Roy (1995), which is given by

$$u_b=u+\frac{Q}{B(h+\zeta)}, \tag{15}$$

where Q and B are river discharge and breadth of the river along the longitude, respectively.

4.2 *Discretization of spatial derivatives*

The governing equations given by Eqs (1)–(3) as well as the boundary conditions given by Eqs (6)–(8) are discretized by finite-difference (central) for spatial derivatives only using the well-known Arakawa C-grid by considering the discrete points in

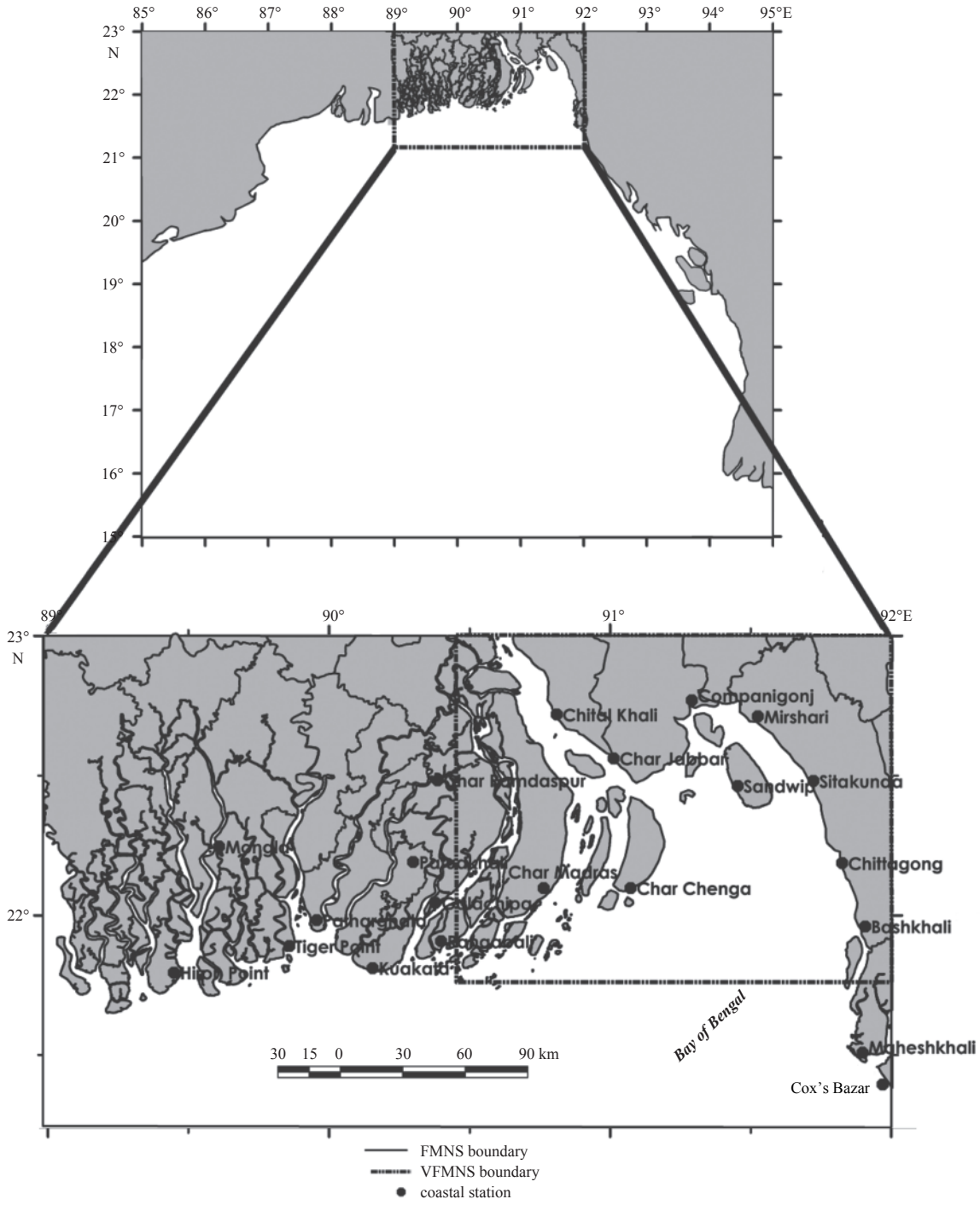

Fig. 1. Domains of the three schemes CMNS, FMNS, and VFMNS with delimited boundaries and actual coastal and island boundaries along with ten representative locations in the VFMNS at which computed results are presented.

Table 1. Domains, grid resolutions and number of computational grid points of used schemes

Scheme	Domain	Grid resolution along *x*-axis	Grid resolution along *y*-axis	Number of computational points
CMNS	15°–23°N and 85°–95°E	15.08 km	17.52 km	60×61
FMNS	21°15–23°N and 89°–92°E	2.15 km	3.29 km	92×95
VFMNS	21.77°–23°N and 90.40°–92°E	720.73 m	1142.39 m	190×145

the xy-plane defined by $x_i=(i-1)\Delta x$, $i=1, 2, 3, ..., M(\text{even})$, $y_j=(j-1)\Delta x$, $j=1, 2, 3, ..., N(\text{odd})$. Since the C-gid system is well-known and hence details of it are not presented here. However, it can be found in Paul and Ismail (2012).

Suppose that $\chi(x, y, t)$ represents any dependent variable at a grid point (x_i, y_j) at time t_k. We define the following operators:

$$\chi\left(x_i, y_j, t_k\right)=\chi_{i,j}^k, \frac{1}{2}(\chi_{i+1,j}^k+\chi_{i-1,j}^k)=\overline{\chi_{i,j}^k}^x,$$

$$\frac{1}{2}(\chi_{i,j+1}^k+\chi_{i,j-1}^k)=\overline{\chi_{i,j}^k}^y, \frac{1}{4}(\chi_{i+1,j}^k+\chi_{i-1,j}^k+\chi_{i,j+1}^k+\chi_{i,j-1}^k)=\overline{\chi_{i,j}^k}^{xy}.$$

Then Eqs (1)–(3) can be written, respectively, as follows:

$$\left(\frac{\partial \zeta}{\partial t}\right)_{i,j}=CR1+CR2, \tag{16}$$

where $i=2, 4, ..., M-2$ and $j=3, 5, ..., N-2$.

$$\left(\frac{\partial u}{\partial t}\right)_{i,j}=UR1+UR2+UR3+UR4+UR5+UR6, \tag{17}$$

where $i=3, 5, ..., M-1$ and $j=3, 5, ..., N-2$.

$$\left(\frac{\partial v}{\partial t}\right)_{i,j}=VR1+VR2+VR3+VR4+VR5+VR6, \tag{18}$$

where $i=2, 4, ..., M-2$ and $j=2, 4, ..., N-1$.

In Eqs (16)–(18),

$$CR1=-\frac{(\overline{\zeta_{i+1,j}^k}^x+h_{i+1,j})u_{i+1,j}^k-(\overline{\zeta_{i-1,j}^k}^x+h_{i-1,j})u_{i-1,j}^k}{2\Delta x},$$

$$CR2=-\frac{(\overline{\zeta_{i,j+1}^k}^y+h_{i,j+1})v_{i,j+1}^k-(\overline{\zeta_{i,j-1}^k}^y+h_{i,j-1})v_{i,j-1}^k}{2\Delta y},$$

$$UR1=-\begin{cases}u_{i,j}^k\dfrac{u_{i+2,j}^k-u_{i-2,j}^k}{4\Delta x}, & \text{for } i\neq m-1\\ u_{i,j}^k\dfrac{0.5(3u_{i,j}^k-u_{i-2,j}^k)-u_{i-2,j}^k}{4\Delta x}, & \text{for } i=m-1\end{cases}$$

$$UR2=-\overline{v_{i,\cdots j}^k}^{xy}\frac{\overline{u_{i,j+1}^k}^y-\overline{u_{i,j-1}^k}^y}{2\Delta y}, UR3=f_{i,j}\overline{v_{i,j}^k}^{xy}, UR4=-g\frac{\zeta_{i+1,j}^{k+1}-\zeta_{i-1,j}^{k+1}}{2\Delta x},$$

$$UR5=\frac{T_x}{\rho(\overline{\zeta_{i,j}^{k+1}}^x+h_{i,j})}, UR6=-\frac{C_f u_{i,j}^k}{\overline{\zeta_{i,j}^{k+1}}^x+h_{i,j}}\left[\left(u_{i,j}^k\right)^2+\left(\overline{v_{i,j}^k}^{xy}\right)^2\right]^{1/2},$$

$$VR1=-\begin{cases}\overline{u_{i,j}^k}^{xy}\dfrac{\overline{v_{i+1,j}^k}^x-\overline{v_{i-1,j}^k}^x}{2\Delta x}, & \text{for } i\neq 2\\ \overline{u_{i,j}^k}^{xy}\dfrac{\overline{v_{i+1,j}^k}^x-0.5(3v_{i,j}^k-v_{i+2,j}^k)}{2\Delta x}, & \text{for } i=2\end{cases}$$

$$VR2=-\begin{cases}v_{i,j}^k\dfrac{v_{i,j+2}^k-v_{i,j-2}^k}{4\Delta y}, & \text{for } j\neq 2, j\neq n-1\\ v_{i,j}^k\dfrac{v_{i,j+2}^k-0.5(3v_{i,j}^k-v_{i,j+2}^k)}{4\Delta y}, & \text{for } j=2\\ v_{i,j}^k\dfrac{0.5(3v_{i,j}^k-v_{i,j-2}^k)-v_{i,j-2}^k}{4\Delta y}, & \text{for } j=n-1\end{cases}$$

$$VR3=-f_{i,j}\overline{u_{i,j}^k}^{xy}, VR4=-g\frac{\zeta_{i,j+1}^{k+1}-\zeta_{i,j-1}^{k+1}}{2\Delta y}, VR5=\frac{T_y}{\rho(\overline{\zeta_{i,j}^{k+1}}^y+h_{i,j})}$$

and

$$VR6=-\frac{C_f v_{i,j}^k}{\overline{\zeta_{i,j}^{k+1}}^y+h_{i,j}}\left[\left(\overline{u_{i,j}^k}^{xy}\right)^2+\left(v_{i,j}^k\right)^2\right]^{1/2}.$$

From the boundary conditions given by Eqs (6)–(8), the elevations at j=1 (western), j=N (eastern) and i=M (southern) are computed, respectively, in the following manner.

$$\zeta_{i,1}^{k+1}=-\zeta_{i,3}^{k+1}-2\sqrt{(h_{i,2}/g)}\,v_{i,2}^k, \tag{19}$$

$$\zeta_{i,N}^{k+1}=-\zeta_{i,N-2}^{k+1}+2\sqrt{(h_{i,,\ N-1}/g)}\,v_{i,N-1}^k, \tag{20}$$

$$\zeta_{M,j}^{k+1}=-\zeta_{M-2,\cdots j}^{k+1}+2\sqrt{(h_{M-1,j}/g)}u_{M-1,j}^k. \tag{21}$$

where i=2, 4, 6, ..., M–2 and j=1, 3, 5, 7, ..., N.

The discretized equations presented above are also addressed in Paul et al. (2014), but due to subsequent relevant convenience, they are also presented in the study.

4.3 *Data set up and initial conditions*

The input data in our study are collected and compiled from various sources. The map of the study area was made with Google My Maps through ArcGIS software with which the three schemes, namely CMNS, FMNS, and VFMNS were created. The schemes were digitized according to their resolutions and were made usable for implementing our proposed method following an algorithm addressed in Murshed et al. (2016). The required meteorological inputs, namely maximum sustained wind speed, maximum sustained wind radius, and storm track (Fig. 2) were obtained from the BMD. It is to be mentioned here that the data related to the storm April 1991 were collected, as the numerical experiments which were performed with this storm. For specifying water depth data at the grid points of our used schemes, firstly a contour map for the region of interest is made from the British Admiralty Chart. Then from that contour map, an interpolated bathymetry is generated using Shepard interpolation with the help of a Matlab program. Contours of our interpolated bathymetry are delineated in Fig. 3. Water depth data at the grid points of the used three schemes are compiled using again the same interpolation with the use of that interpolated bathymetry. In our numerical calculations, we have used C_f=0.002 6, C_D=0.002 8 (see Paul et al., 2016), Q=5 100.0 m^3/s (Jain et al., 2007). The initial values of ζ, u and v are taken as zero to represent a cold start. An initial time step of 60 seconds is used that ensures Courant–Friedrichs–Lewy (CFL) stability criterion. The rest of the parameters involved in the problem have been assumed to have their standard values.

4.4 *Solution by the novel RKARMS (4, 4) technique*

For every grid point (x_i, y_j), one can see Eq. (16) to have the following form with *CR*1 and *CR*2:

$$\left(\frac{\partial \zeta}{\partial t}\right)_{i,j}=f_1(\zeta_{l,m}^k, u_{l,m}^k, v_{l,m}^k, h_{l,m}), \tag{22}$$

where $l=i-1, i, i+1; m=j-1,\ j,\ j+1$; $i=2, 4, ..., M-2$ and j = 3, 5, ..., N – 2.

Again, for every grid point (x_i, y_j), where i=3, 5, ..., M – 1 and j=3, 5, ..., N – 2, Eq. (17) can be written as

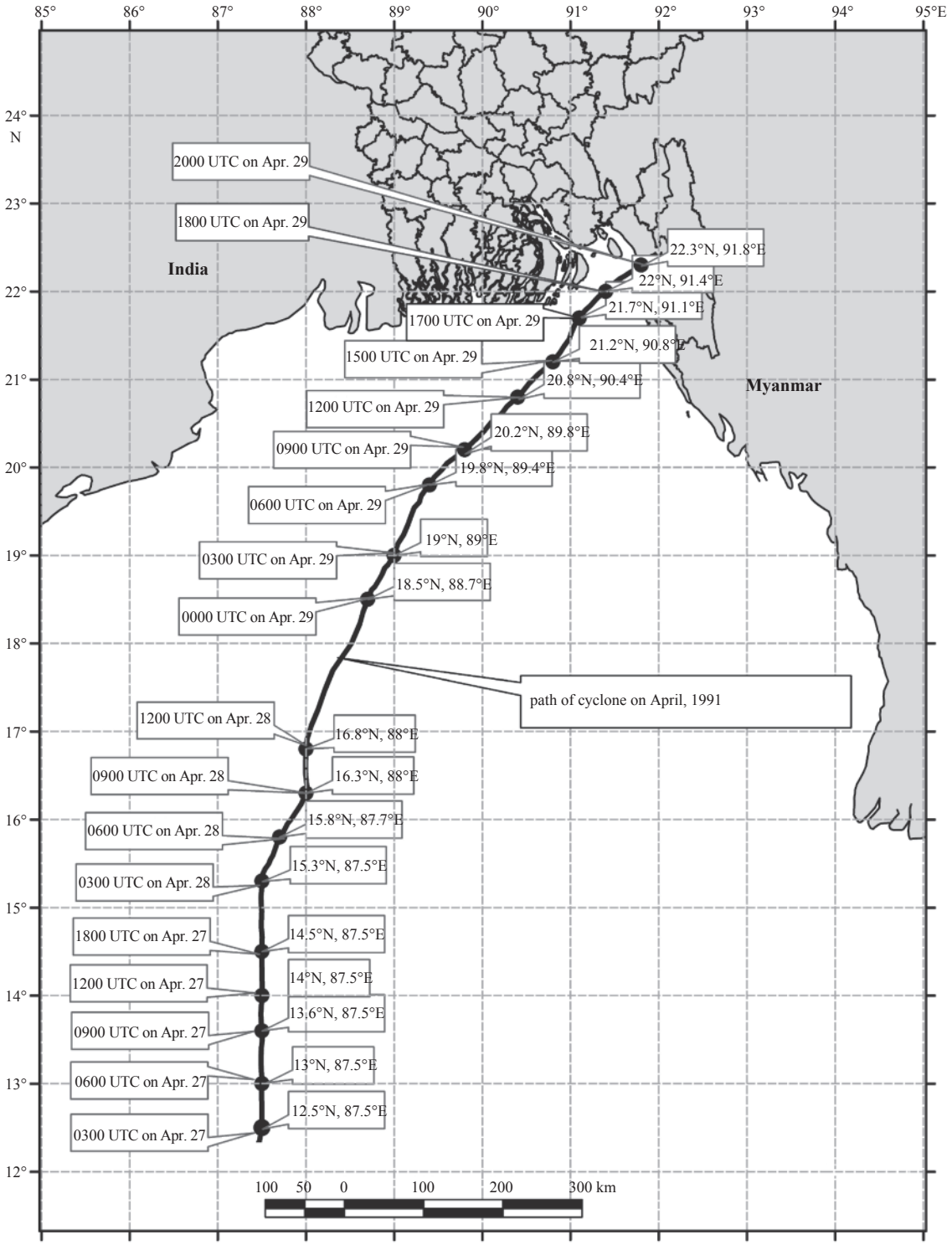

Fig. 2. Track of the cyclone April 1991 (Adopted from the study of Paul et al., 2016).

$$\left(\frac{\partial u}{\partial t}\right)_{i,j} = f_2(\zeta_{l,m}^{k+1}, u_{l,m}^{k}, v_{l,m}^{k}, h_{l,m}), \tag{23}$$

where $l = i-2, i-1, i, i+1, i+2$ and $m = j-2, j-1, j, j+1, j+2$.

Finally, for every grid point (x_j, y_j), Eq. (18) can be written as

$$\left(\frac{\partial v}{\partial t}\right)_{i,j} = f_3(\zeta_{l,m}^{k+1}, u_{l,m}^{k}, v_{l,m}^{k}, h_{l,m}), \tag{24}$$

where $l = i-2, i-1, i, i+1, i+2$; $m = j-2,\ j-1,\ j,\ j+1,\ j+2$; $i = 2, 4, \ldots, M-2$ and $j = 2, 4, \ldots, N-1$.

In Eqs (22)–(24), the superscripts k and k+1 indicate the values of the variable at kth and (k+1)th time levels, respectively. The known values of $\zeta_{l,m}^{k}\zeta_{l,m}^{k}$, $\zeta_{l,m}^{k+1}$, $u_{l,m}^{k}$, $v_{l,m}^{k}$ and $h_{l,m}$ on the right hand side of Eqs (22)–(24) are used as the initial conditions for integrating the corresponding equation at every time instant. Firstly, Eq. (22) with the initial conditions of the variables in-

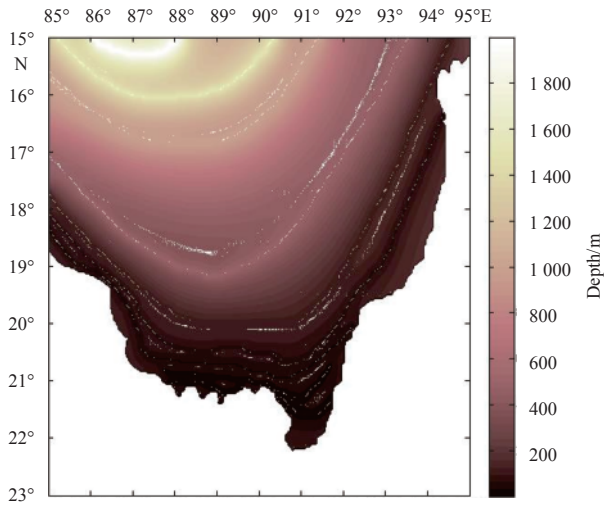

Fig. 3. Contours of our interpolated bathymetry using Shepard interpolation.

volved (discussed in Subsection 4.3) is solved with the help of the novel RKARMS (4, 4) method to update the values of ζ at the interior points, Eqs (19)–(21) are then used to upgrade the values of ζ at the boundary points. Finally, average procedure is adopted to get elevations at the remaining grid points representing water and coastal or island boundaries. Track of the cyclone is then generated with the obtained data from the BMD, associated wind field is generated subsequently using Eqs (4) and (5). Equation (23) is then integrated by the novel RKARMS (4, 4) technique and finally Eq. (24) is solved. The procedure is repeated over time updating the values of the variables ζ , u, and v at each time step of the solution process. The same procedure is employed to all the schemes, where the only difference is in the boundaries. There are three open boundaries of the CMNS, where a condition of radiation type given by Eqs (19)–(21) is applied. The results along three particular grid lines of the CMNS are coupled with those of the open boundaries of the FMNS. The grid lines of the CMNS which are adjacent to those of the FMNS are chosen. The coupling of the schemes is made by a weighted interpolation. A similar manner is adopted in coupling the FMNS and VFMNS. Along the northern side of the VFMNS, u_b is computed at points (1, j) using Eq. (15) in which u on the RHS is replaced by $u_{3,j}$, where j = 7, 9, 11, 13, 15, 17, 19.

5 Results and discussion

It is aforementioned that our numerical experiments were carried out with the April 1991 cyclone as it crossed the coast over the analysis area. For analysis of results, the time history of the storm is of help. The details of it are addressed in Paul et al. (2016), and hence it is not presented in this study. But for convenience, the track of the storm and the corresponding table are presented here (Fig. 2 and Table 2), where the data were received from the BMD. The results were calculated for 72 h and the water levels at some grid points representing representative stations were presented for the last 48 h for better perspective.

Figures 4 and 5 depict our model simulated surge levels associated with the cyclone April 1991 at some locations in the analysis area. It can be seen from the figure that our simulated maximum surge levels in this area vary between 5.16–7.03 m and the surge level at Chittagong is found to be 5.39. Rahman et al. (2013) estimated 4.04–6.01 m surge along the Meghna estuarine region, Paul et al. (2014) predicted 5–7 m high surge in this area, Paul et al. (2016) estimated a storm surge of 6–8 m along the estuary of Meghna, whereas Dube et al. (2004) computed a peak surge value of 5.8 m at Chittagong. By a report from the BMD, the maximum surge level at Chittagong was 5.5 m and there was 3.5–6.1 m surge along the coast of Bangladesh (Paul et al., 2014). Thus our computed peak surge values in our region of interest are in a reasonable agreement with those obtained in different investigations and the peak surge value at Chittagong compares well with the reported surge height by the BMD. According to a report from the BMD, the cyclone made landfall near the north of Chittagong coast (at Companigonj) about 20: 00 UTC on April 29. Our simulated results presented in Fig. 4 justify the landfall time of the storm. As the astronomical tide is not considered here in the study, so the estimated land fall time may vary. It is pertinent to point out here that astronomical tides cannot be found switched off in the nature and therefore one cannot observe a surge and hence comparison of our time variation of surge levels with observation is not done. Surge levels (Figs 4 and 5) around Chittagong were found to be higher than that of the levels at other

Table 2. The positions and the nature of the April 1991 cyclone with varying time (Source: BMD)

Date	Hour (UTC)	North latitude	East longitude	Nature of the storm
Apr. 25	0003	10.00°	89.00°	depression
Apr. 25	1200	11.50°	88.50°	deep depression
Apr. 25	1800	11.80°	88.50°	cyclonic storm
Apr. 26	1800	11.00°	87.50°	cyclonic storm
Apr. 27	0000	11.80°	87.50°	cyclonic storm
Apr. 27	0900	12.50°	87.50°	cyclonic storm
Apr. 27	1200	13.00°	87.50°	cyclonic storm
Apr. 27	1500	13.60°	87.50°	severe cyclonic storm
Apr. 28	0000	14.50°	87.50°	severe cyclonic storm with hurricane core
Apr. 28	1200	15.80°	87.70°	severe cyclonic storm with hurricane core
Apr. 28	1400	16.50°	88.00°	severe cyclonic storm with hurricane core
Apr. 29	0000	17.60°	88.30°	severe cyclonic storm with hurricane core
Apr. 29	1200	19.80°	88.40°	severe cyclonic storm with hurricane core
Apr. 29	1800	20.80°	88.50°	severe cyclonic storm with hurricane core
Apr. 30	0000	22.00°	91.00°	severe cyclonic storm with hurricane core
Apr. 30	0200	22.30°	92.80°	severe cyclonic storm with hurricane core

Note: The maximum wind speed is 234 km/h, and the maximum radius of sustained wind is 50 km.

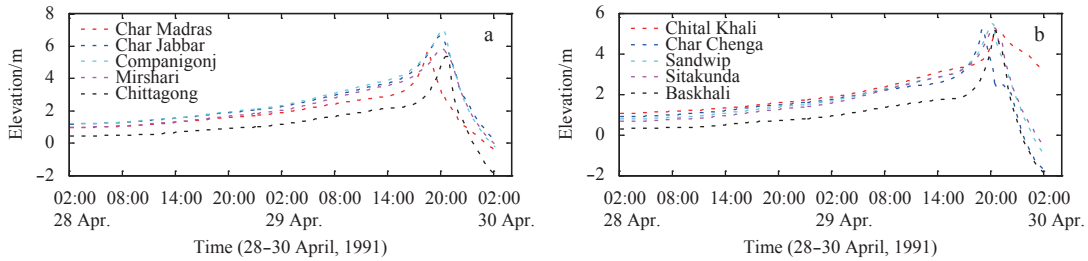

Fig. 4. Time variation of computed water levels with respect to the mean sea level (MSL) due to surge in the absence of astronomical tide at some coastal and island locations in the Meghna Estuary.

locations of the estuary. This is as to be expected as the storm crossed the coast at Companigonj, which is just north of Chittagong (Paul and Ismail, 2013) and may be this is the reason of highest surge value (7.03 m) at Companigonj (Figs 2 and 4a), which is supported by Flather (1994). It can be seen from Fig. 4 that the maximum surge level at each location increase with time as the storm approaches the coast and finally there is a recession. This is expected as the circulatory wind attains highest intensity during crossing the coast. A similar analysis can be found to make in some investigations, namely Paul and Ismail (2012, 2013) and Paul et al. (2014, 2016). The beginning of recession at the coastal locations delays with the increase in their east longitudes (Fig. 4). The track of the cyclone may be one of the reasons behind the fact.

The study was also conducted employing the FDM (forward in time and central in space) as well as employing the MOL in coordination with the RK (4, 4) method using the same nested schemes, same grid, same coupling system of the schemes, same set of equations with same boundary conditions and same values for the parameters that were used in the case of the present study. Figure 5 provides a comparison of time variation of water levels due to surge simulated by the present study and the other two methods of interest at Char Chenga, Chittagong and Sandwip. Figure 5 shows that surge levels simulated by our model compare well with the ones computed by the FDM and by employing the MOL in coordination with the RK (4, 4) method. Surge levels computed by our model for other locations of the estuary also compared well with the ones computed by the said two methods. Other such figures are excluded due to the sake of brevity.

To test the effect of Meghna River fresh water discharge, grid resolution, Coriolis force and offshore islands on surge levels, the model was run without including each of the factors namely, the river discharge, VFMNS scheme, Coriolis force and offshore islands keeping all other factors fixed. The results for the peak surge values are presented in Fig. 6. It can be seen from the figure that the region's surge levels are modified by the offshore islands and Coriolis force. It can also be inferred from the figure that surge levels increase at each of the stations when discharge is taken into account and the resolution of grids can be a factor for foreseeing surge levels accurately in the area of interest. To investigate the contribution of water depth on surge levels, the model is run with a constant water depth of 10 m. The peak surge values in this regard are also presented in Fig. 6. In that case water levels were found to be amplified. Thus for proper estimation of surge levels, water depth should properly be taken into account.

In our computation, initial time step size, Δt, is used as 60 s. Although, we have presented our results taking time step Δt as 60 s,

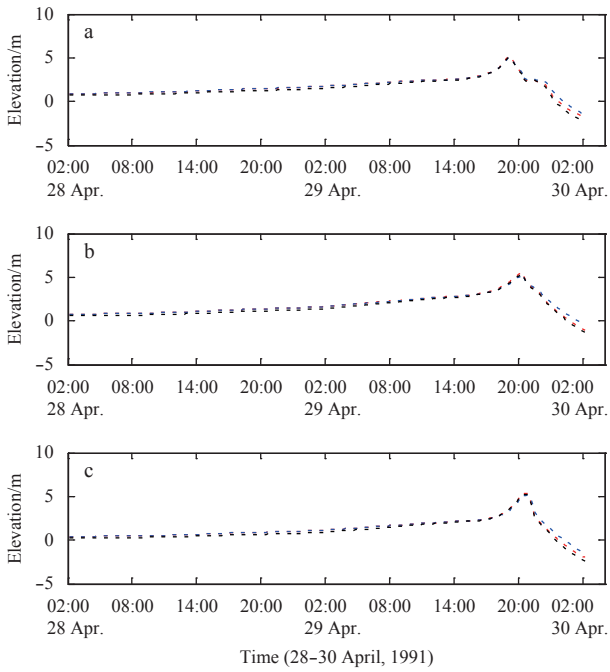

Fig. 5. Comparison of our simulated surge levels with respect to the MSL by the present study with that obtained by the MOL in coordination with the RK (4, 4) method and the FDM at Char Chenga (a), Sandwip (b) and Chittagong (c). In each case, a dotted red curve represents configuration for time variation of water levels obtained by the present study, a blue dotted curve that for the MOL in addition with RK (4, 4) method and a dotted black curve that for the FDM.

we have also computed our results taking different time steps, namely 90 s, 30 s, 20 s, and 10 s. The results obtained employing the MOL in coordination with both the RKARMS (4, 4) and RK (4, 4) methods in each case generally agreed the results presented in each case and no numerical instability was achieved. But the FDM failed to ensure stability for some time steps mentioned above. In order to compare the computational efficiency of the methods, the codes were run on the same computer with initial time step 60 s. The computational time in the case of the present study was found to be a little bit more in comparison with the other two, but with the use of higher time step it can be reduced, as no numerical instability was obtained with higher time step in the case of the present study and there is a facility of controlling step size automatically based on the LTE by the method.

Further development is yet to be made with respect to its refinement and inclusion of astronomical tide. It is pertinent to

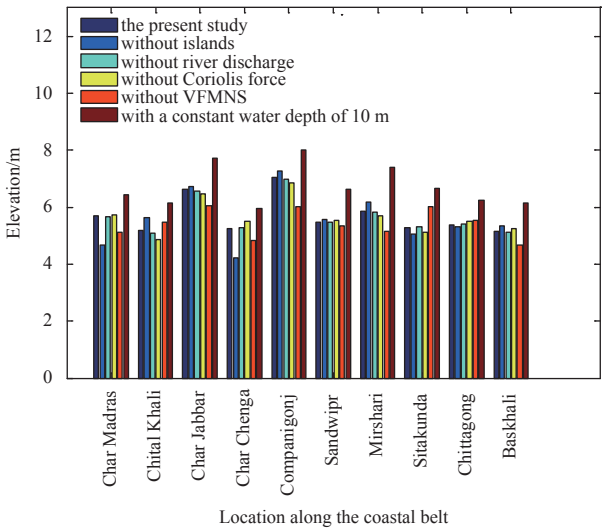

Fig. 6. Computed peak surge values by the present study and without including each of the factors, namely islands, river discharge, VFMNS, and Coriolis force keeping the other factors unchanged. Peak water levels with a constant water depth of 10 m is also presented in the figure.

pinpoint out here that tide can be generated by the cubic spline interpolation with the available hourly tidal data from the BIWTA and that can be added with time variation pure surge values obtained in the study to obtain the total water levels. Since our main intention was to solve SWEs by the new different approach adopted in this study, astronomical tide was not incorporated.

6 Conclusions

Ensuring robustness of the solutions is essential through new RKARMS (4, 4) method if the significant practical benefits of vertically integrated SWEs in Cartesian coordinates are solved using the MOL to predict water levels due to surge along the world's most vulnerable region, the Meghna Estuary. The region's surge levels are found to be influenced by some factors, namely river discharge, grid resolution, offshore islands, water depth and Coriolis force. Thus for prediction of surge levels with a considerable accuracy along the region of interest, one needs to incorporate the above factors properly in a model with a precise understanding of the factors. However, simulated surge levels by the study are found to be in good agreement with some reported data and are found to compare well in comparison with the results obtained by the FDM and the MOL in coordination with the RK (4, 4) method. Indeed, the MOL approach minimizes computational effort and cost. It has the advantages of computational efficiency, numerical stability and a significant benefit of using sophisticated ODE integrator. On the other hand, RKARMS (4, 4) can control step size based on the LTE, which in turn can reduce computational cost. Hence the method adopted in the study can be an alternative approach for the prediction of surge levels associated with a storm along the coast of Bangladesh.

Acknowledgements

The authors are thankful to the anonymous reviewers for their insightful comments in improving the quality of the manuscript. The first author would like to thank Md. Mizanur Rahman, from Department of Mathematics, Shahjalal University of Science & Technology, Sylhet, Bangladesh for providing necessary data and Figures. The second author would like to extend his sincere gratitude to Professor Ramasamy Ponalagusamy, Department of Mathematics, National Institute of Technology [REC], Tiruchirappalli-620015, Tamilnadu, India for his valuable guidance during doctoral research work. Rana Pria is an M.Sc. student of Mathematics Discipline, Khulna University, Bangladesh, who would like to thank her supervisor for his valuable suggestions.

References

Das P K. 1972. Prediction model for storm surges in the Bay of Bengal. Nature, 239(5369): 211–213

Debsarma S K. 2009. Simulations of storm surges in the Bay of Bengal. Marine Geodesy, 32(2): 178–198

Dube S K, Chittibabu P, Sinha P C, et al. 2004. Numerical modelling of storm surge in the head Bay of Bengal using location specific model. Natural Hazards, 31(2): 437–453

Evans D J, Yaakub A R. 1995. A new Runge Kutta RK(4,4) method. International Journal of Computer Mathematics, 58(3–4): 169–187

Fehlberg E. 1969. Low-order classical Runge-Kutta formulas with stepsize control and their application to some heat transfer problems. NASA TR R-315, Washington D C: NASA

Flather R A. 1994. A storm surge prediction model for the northern Bay of Bengal with application to the cyclone disaster in April 1991. Journal of Physical Oceanography, 24(1): 172–190

Ismail A I M, Karim F, Roy G D, et al. 2007. Numerical modelling of tsunami via the method of lines. World Academy of Science, Engineering and Technology, 32: 177–185

Jain S K, Agarwal P K, Singh V P. 2007. Hydrology and Water Resources of India. Netherlands: Springer, 308

Jelesnianski C P. 1965. A numerical calculation of storm tides induced by a tropical storm impinging on a continental shelf. Monthly Weather Review, 93(6): 343–358

Merson R H. 1957. An Operational Method for The Study of Integration Processes. In: Proceedings of a Symposium on Data Processing. Salisbury, South Australia: Weapons Research Establishment

Murshed M M, Paul G C, Haque M R. 2016. On the approximation of complex geometric domain to be compatible for the implementation of finite difference method. International Journal of Scientific & Engineering Research, 7(5): 495–501

Paul G C, Ismail A I M. 2012. Numerical modeling of storm surges with air bubble effects along the coast of Bangladesh. Ocean Engineering, 42: 188–194

Paul G C, Ismail A I M. 2013. Contribution of offshore islands in the prediction of water levels due to tide–surge interaction for the coastal region of Bangladesh. Natural Hazards, 65(1): 13–25

Paul G C, Ismail A I M, Karim M F. 2014. Implementation of method of lines to predict water levels due to a storm along the coastal region of Bangladesh. Journal of Oceanography, 70(3): 199–210

Paul G C, Ismail A I M, Rahman A, Karim M F, Hoque A. 2016. Development of tide–surge interaction model for the coastal region of Bangladesh. Estuaries and Coasts, 39(6): 1582–1599

Paul G C, Senthilkumar S. 2016. Execution of novel explicit RKARMS(4,4) technique in determining initial configurations of extra-solar protoplanets formed by disk instability. NRIAG Journal of Astronomy and Geophysics, 5(1): 1–8

Ponalagusamy R, Senthilkumar S. 2009. A new method of embedded fourth order with four stages to study raster CNN simulation. International Journal of Automation and Computing, 6(3): 285–294

Rahman M M, Paul G C, Hoque A. 2013. Nested numerical scheme in a polar coordinate shallow water model for the coast of Bangladesh. Journal of Coastal Conservation, 17(1): 37–47

Roy G D. 1995. Estimation of expected maximum possible water level along the Meghna estuary using a tide and surge interaction model. Environment International, 21(5): 671–677

Roy G D, Kabir A B M H, Mandal M M, et al. 1999. Polar coordinates shallow water storm surge model for the coast of Bangladesh. Dynamics of Atmospheres and Oceans, 29(2–4): 397–413

Sadiku M N O, Garcia R C. 2000. Method of lines solution of axisymmetric problems. In: Proceedings of the IEEE Southeastcon, Nashville, TN, USA: IEEE, 527–530

Senthilkumar S. 2009. New embedded Runge-Kutta fourth order four stage algorithms for raster and time-multiplexing cellular neural networks simulation[dissertation]. Tiruchirappalli, Tamilnadu, India: National Institute of Technology

Sun Weikai, Wang Yunyi, Zhu Weigang. 1993. Analysis of waveguide inserted by a metallic sheet of arbitrary shape with the method of lines. International Journal of Infrared and Millimeter Waves, 14(10): 2069–2084

Yaacob N, Sanugi B. 1998. A new fourth-order embedded method based on the harmonic mean. Matematika, 14: 1–6

Yaakub A R, Evans D J. 1999. A fourth order Runge-Kutta RK(4,4) method with error control. International Journal of Computer Mathematics, 71(3): 383–411